Pictorial Essay

Lung Masses of Unusual Histologies Mimicking Malignancy: Flurodeoxyglucose Positron Emission Tomography-Computed Tomography Appearance

Abstract

18F flurodeoxyglucose positron emission tomography-computed tomography (18F FDG PET-CT) is widely used in the evaluation of patients with lung mass suspicious for malignancy. In addition to malignancy, a variety of benign neoplasms and inflammatory lesions can arise in the lungs, many of which show increased FDG concentration, thereby mimicking malignancy. Awareness of the common mimics of lung cancer and a thorough understanding of their key imaging characteristics on CT as well as FDG PET is helpful in narrowing the differential diagnosis, eventually leading to appropriate therapy. In this article, we enlist these mimics and discuss their metabolic and morphologic characteristics and provide a pathophysiological basis for their FDG uptake.

Keywords: *18F flurodeoxyglucose positron emission tomography-computed tomography, lung mass, mimicking malignancy, unusual histologies*

Boon Mathew, Nilendu C Purandare, Sneha Shah, Ameya Puranik, Archi Agrawal, Venkatesh Rangarajan

Department of Nuclear Medicine and Molecular Imaging, Tata Memorial Hospital, Homi Bhabha National Institute, Mumbai, Maharashtra, India

Introduction

18F flurodeoxyglucose positron emission tomography-computed tomography (18F FDG PET-CT) is an established modality in the evaluation of lung masses, especially in patients with suspected carcinoma lung.[1] A variety of benign neoplasms and inflammatory lesions can arise in the lungs, many of which show increased FDG concentration, thereby mimicking malignancy. In this article, we enlist these mimics [Table 1] and discuss their metabolic and morphologic characteristics and provide a pathophysiological basis for their FDG uptake.

Tuberculosis

Tuberculosis is a chronic granulomatous infection caused by *Mycobacterium tuberculosis*. Common patterns described on CT scan are tree in bud opacities, cavitatory lesions, and nodules with a central hypoenhancing necrotic area with peripheral enhancing rim of granulomatous inflammatory zone.[2] Active tuberculous lesions involving lung parenchyma usually show high FDG uptake [Figure 1]. It is due to the high glycolytic rate of a large number of activated macrophages seen in these lesions.[3] Thick-walled cavities with high FDG uptake mimicking squamous carcinoma are also seen in pulmonary tuberculosis, making a diagnosis of lung cancer difficult.

Organizing Pneumonia

Focal organizing pneumonia is considered as unresolving pneumonia or pneumonia with delayed resolution. It consists of a granulation tissue with chronic inflammatory cell infiltrate. On CT, it appears as an area of consolidation or a nodule with spindle-shaped margins and satellite nodules.[4] Sometimes, it appears as a nodule or mass with spiculated margins and central necrosis, resembling malignant lung pathology. As these lesions contain inflammatory cells with upregulated glucose metabolism, they show FDG uptake [Figure 2].[5]

Sarcoidosis

Sarcoidosis is a multisystem disease of unknown etiology which can affect any organ in the body. Mediastinal and hilar lymph node involvement is the most common finding, followed by lung parenchymal involvement. Typical CT findings of lung involvement are

How to cite this article: Mathew B, Purandare NC, Shah S, Puranik A, Agrawal A, Rangarajan V. Lung masses of unusual histologies mimicking malignancy: Flurodeoxyglucose positron emission tomography-computed tomography appearance. Indian J Nucl Med 2019;34:295-301.

Address for correspondence:
Dr. Nilendu C Purandare, Department of Nuclear Medicine and Molecular Imaging, Tata Memorial Hospital, Parel, Mumbai - 400 012, Maharashtra, India.
E-mail: nilpurandare@gmail.com

Access this article online

Website: www.ijnm.in

DOI: 10.4103/ijnm.IJNM_116_19

Quick Response Code:

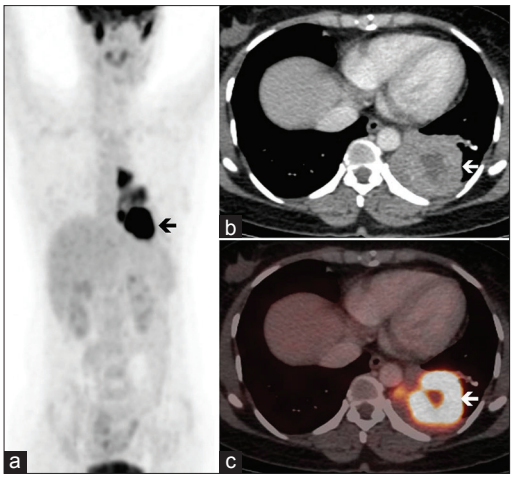

Figure 1: Tuberculosis: A 43-year-old woman with complaints of cough and loss of weight. Flurodeoxyglucose positron emission tomography-computed tomography whole-body maximum intensity projection image (a) shows intense flurodeoxyglucose uptake in the left side of thorax (arrow). Axial computed tomography image (b) shows a left lung mass with irregular margins, peripheral enhancement, and central necrosis (arrow). Axial fusion image (c) shows intense flurodeoxyglucose uptake in the left lung mass (arrow). Histopathologic examination revealed central caseation surrounded by epithelioid cell granulomas, favoring tuberculosis

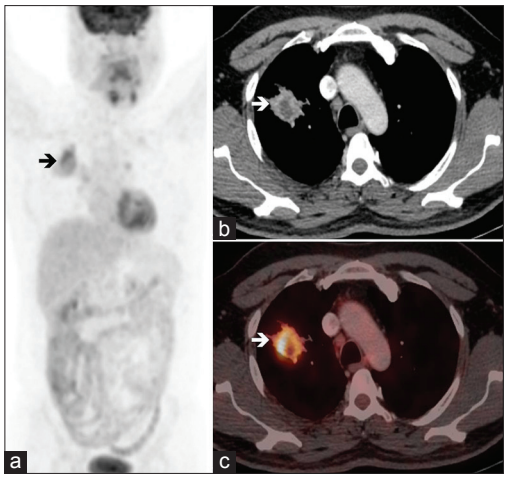

Figure 2: Organizing pneumonia: A 60-year-old gentleman with complaints of right-sided chest pain, cough, and hemoptysis. Flurodeoxyglucose positron emission tomography-computed tomography whole-body maximum intensity projection image (a) shows flurodeoxyglucose uptake in the right side of thorax (arrow). Axial computed tomography image (b) shows a right lung nodule with irregular margins, peripheral enhancement, and central necrosis (arrow). Axial fusion image (c) shows intense flurodeoxyglucose uptake in the right lung nodule (arrow). Histopathologic examination revealed inflamed lung parenchyma with areas of acute inflammation and granulation tissue surrounded by dense chronic plasma cell inflammation and fibrosis, suggestive of organizing pneumonia

Table 1: Flurodeoxyglucose avid and nonavid lung masses

FDG avid	FDG nonavid/low grade avid
Tuberculosis	Pulmonary sequestration
Organizing pneumonia	Schwannoma
Sarcoidosis	Hamartoma
Aspergillosis	Solitary fibrous tumor
Mucormycosis	Benign PEComa
Wegener's granulomatosis	Pleomorphic adenoma
Inflammatory myofibroblastic tumor	Carcinoid
Malignant PEComa	
Castleman disease	

PEComa: Perivascular epitheliod cell tumor, FDG: Flurodeoxyglucose

bilateral perihilar opacities, micronodules showing peribronchovascular distribution, and fibrotic changes. Few cases may show atypical manifestations such as miliary opacities, mass-like or alveolar opacities, honeycomb-like cysts, tracheobronchial involvement, and pleural disease.[6] On FDG PET, active sarcoid lesions show intense uptake and a nodule or mass-like opacity can resemble malignancy [Figure 3]. Noncaseating granulomas and inflammatory cells including activated macrophages, lymphocytes, and neutrophils are responsible for the accumulation of FDG.[7]

Aspergillosis

Aspergillosis is a mycotic infection caused by *Aspergillus* fungus. It typically affects weakened or damaged lungs or patients with immunodeficiency. *Aspergillus* can colonize a preexisting cavity and grow within the cavity to form an aspergilloma. The mass within the cavity is mobile and lies on the dependent part of the cavity, thus helping to distinguish from a cavitating neoplasm.[8] On CT, it appears as a nodular area or mass-like consolidation with radiolucency within (crescent sign) or surrounded by a zone of low attenuation (halo sign). These lesions contain inflammatory cells and granulation tissue with upregulated glucose metabolism and show good FDG concentration [Figure 4].[9]

Mucormycosis

Mucormycosis is an opportunistic fungal infection caused by the *Rhizopus* genus. Pulmonary mucormycosis is one of the common clinical manifestations of mucormycosis infection. On CT, it may appear as an area of consolidation, nodule, or mass lesion with halo sign or reverse halo sign. Central necrosis with development of air crescent sign is seen in later stages.[10] These lesions are positive on FDG PET as they contains activated inflammatory cells and granulation tissue [Figure 5].[11]

Wegener Granulomatosis

Wegener granulomatosis is an uncommon chronic granulomatous necrotizing vasculitis that involves mainly small- and medium-sized vessels. Pulmonary involvement often predominates and the common CT findings include waxing and waning parenchymal nodules and mass lesions. Other findings include consolidation, cavitary lesions, ground-glass opacities, circumferential tracheobronchial thickening, and pleural effusion.[12] Halo sign and reverse halo sign may also occur in lesions with associated

hemorrhage.[13] Wegener's granulomatosis nodules and cavities may be easily mistaken for lung primary or metastases. Because it is an inflammatory condition, active lesions show increased FDG uptake as they are composed of acute and chronic inflammatory cells [Figure 6].[14]

Pulmonary Sequestration

Pulmonary sequestration (PS) is a rare congenital malformation in the group of bronchopulmonary foregut malformation. PS is an island of nonfunctioning lung tissue commonly seen on CT in posteromedial portion of lower lobes. It lacks direct connection to the normal tracheobronchial tree or pulmonary artery and has an independent systemic arterial vascular supply often identified on CT.[15] Two forms of PS are described based on their relation to pleura, namely intralobar sequestration and extralobar sequestration. CT typically shows a heterogeneous or homogeneous soft-tissue mass which shows partial or heterogeneous contrast enhancement. FDG PET shows no significant tracer uptake in the soft-tissue mass unless it is complicated by infection [Figure 7].[16]

Schwannoma

Schwannoma is a benign mesenchymal tumor arising from Schwann cells. Schwannomas most commonly affect the posterior mediastinum and present as paravertebral mass with or without bone erosion. Rarely, schwannomas can present as well-circumscribed endobronchial lesions.[17] Contrast CT shows homogeneous enhancement in small schwannomas and more heterogeneous enhancement when there is associated cystic degeneration or hemorrhage.[18] Schwannomas show variable FDG uptake and sometimes show intense uptake as the glucose transporter (GLUT) expression varies widely.[19] Because of this, it is difficult to distinguish between a schwannoma and a malignant tumor precisely by imaging alone [Figure 8].

Hamartoma

Hamartoma is a benign mesenchymal neoplasm composed of cartilage, smooth muscle, connective tissue, and fat, with areas of calcification. Hamartoma is the most common benign tumor of the lung and accounts for 77% of all cases.[20] On CT scan, it appears as a well-defined, smooth,

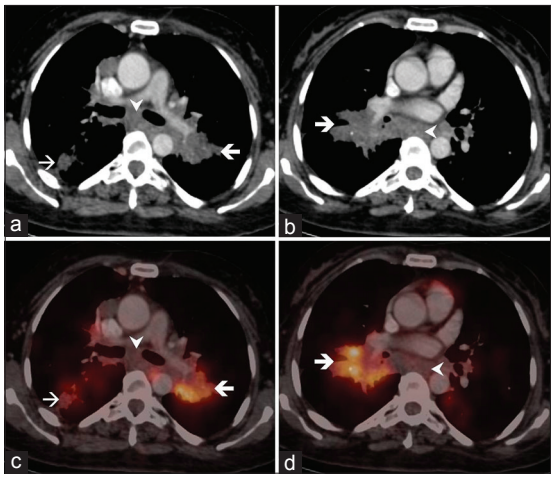

Figure 3: Sarcoidosis: A 34-year-old woman with complaints of dyspnea, cough, and weight loss. Axial computed tomography images (a and b) show bilateral perihilar consolidation (thick arrow), parenchymal nodular lesions (thin arrow), and mediastinal nodes (arrowhead). Axial fusion images (c and d) show flurodeoxyglucose uptake in the perihilar consolidation (thick arrow), parenchymal nodular lesions (thin arrow), and mediastinal nodes (arrowhead). Histopathologic examination revealed chronic nonnecrotizing granulomatous inflammation with epithelioid cell granulomas, favoring sarcoidosis

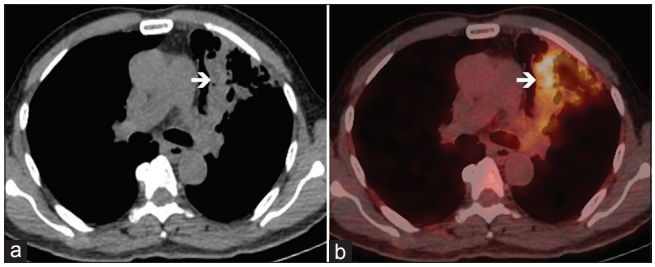

Figure 5: Mucormycosis: A 63-year-old man with complaints of cough with hemoptysis. Axial computed tomography image (a) shows irregular consolidation in the left lung (arrow). Axial fusion image (b) shows good flurodeoxyglucose uptake in the irregular consolidation (arrow). Histopathologic examination revealed abundant fungi with 90° angle branching, consistent with mucormycosis

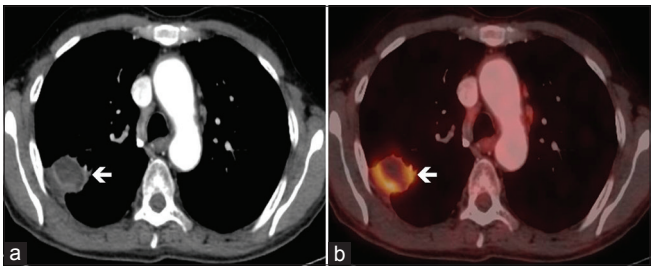

Figure 4: Aspergillosis: A 61-year-old man with complaints of cough with hemoptysis. Axial computed tomography image (a) shows peripheral parenchymal mass in the right lung showing peripheral enhancement and central necrosis (arrow). Axial fusion image (b) shows intense flurodeoxyglucose uptake in the right lung mass (arrow). Histopathologic examination revealed fungal hyphae within a cavitatory lesion lined by histiocytes and other inflammatory cells, suggestive of aspergillosis

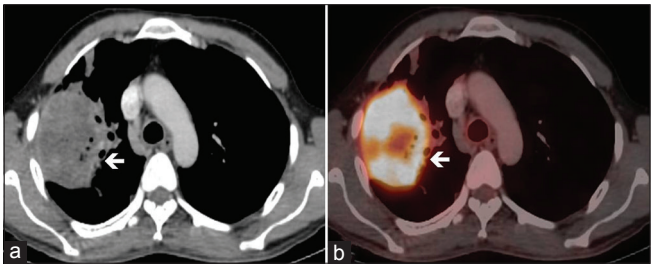

Figure 6: Wegener's granulomatosis: A 46-year-old man with complaints of cough with hemoptysis, loss of appetite, and weight loss. Axial computed tomography image (a) shows mass-like consolidation in the right lung (arrow). Axial fusion image (b) shows flurodeoxyglucose-avid mass-like consolidation in the right lung (arrow). Histopathologic examination revealed necrotizing granulomatous inflammation with polyangiitis, consistent with Wegener's granulomatosis

round, or lobulated nodule or mass lesion, with areas of fatty attenuation. Popcorn calcification or central calcification is seen in about 25% of cases.[20] The presence of intralesional fat and calcification may make the diagnosis of hamartoma easy, but if not identified, it becomes difficult to distinguish from lung cancer or other benign lesions. They usually show low-grade FDG uptake which corresponds to their slow-growing behavior. The mechanism of FDG uptake in hamartomas remains unclear [Figure 9].[21]

Inflammatory Myofibroblastic Tumor

Inflammatory myofibroblastic tumor of lung is a pseudotumor composed of spindle myofibroblasts on a background of collagen and inflammatory cells. Some consider it as a locally invasive low-grade neoplasm and recommends complete surgical excision for definite diagnosis and cure.[22] On CT, it appears as an enhancing, well-defined round/lobulated/spiculated nodule or mass in the peripheral lung parenchyma or occasionally as a well-defined endobronchial lesion. On FDG PET, these tumors usually show very high uptake, which further makes their differentiation from lung cancer difficult.[23] High FDG uptake in these tumors is probably due to the associated intense inflammatory cell infiltration seen [Figure 10].

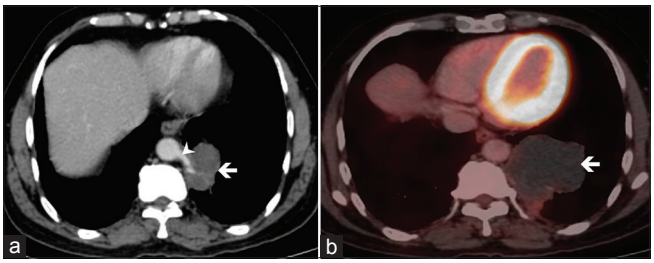

Figure 7: Pulmonary sequestration: A 71-year-old man with incidentally detected left lower-lobe mass on evaluation for right hydronephrosis. Axial computed tomography image (a) shows soft-tissue mass in the left lung (arrow) with feeding vessel arising from thoracic aorta (arrowhead). Axial fusion image (b) shows no flurodeoxyglucose uptake in the left lung mass (arrow). Histopathologic examination revealed benign lung tissue and confirmed the diagnosis of pulmonary sequestration

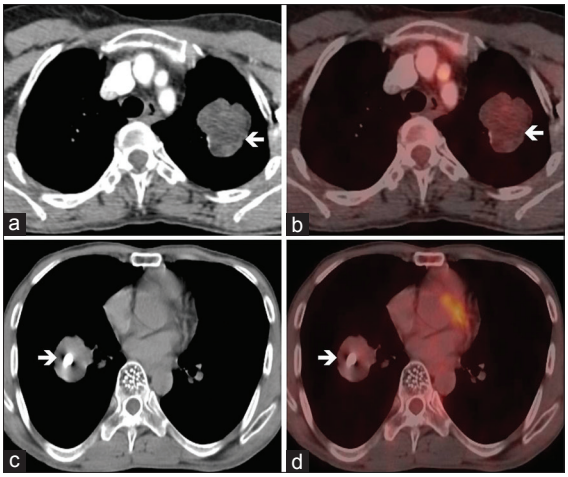

Figure 9: Hamartoma: A 63-year-old woman with complaints of left-sided chest pain. Axial computed tomography image (a) shows a lobulated heterogeneously enhancing soft-tissue mass in the left lung (arrow). Axial fusion image (b) shows low-grade flurodeoxyglucose uptake in the left lung mass (arrow). Histopathologic examination revealed chondroid hamartoma. A 42-year-old man with complaints of cough. Axial computed tomography image (c) shows soft-tissue nodule in the right lung with areas of calcification (arrow). Axial fusion image (d) shows low-grade flurodeoxyglucose uptake in the right lung nodule (arrow). Histopathologic examination revealed chondroid hamartoma

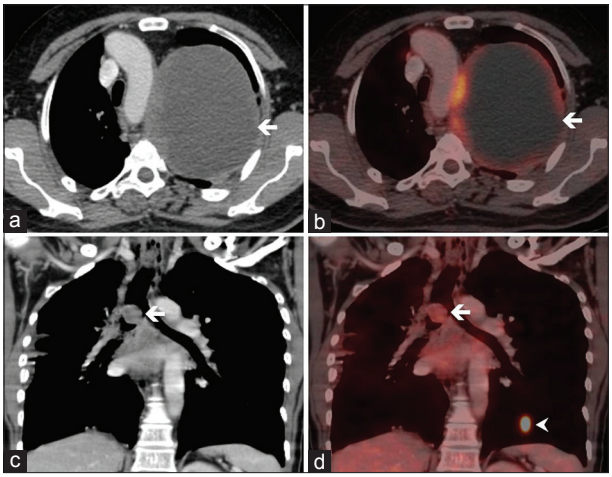

Figure 8: Schwannoma: A 62-year-old man with complaints of dyspnea. Axial computed tomography (a) shows large soft-tissue mass in the left lung (arrow) with peripheral enhancement and central hypodense area. Axial fusion image (b) shows peripheral flurodeoxyglucose uptake with central photopenia in the left lung mass (arrow). Histopathology revealed schwannoma. Endobronchial schwannoma: A 48-year-old woman with complaints of hemoptysis. Axial computed tomography (c) shows endobronchial nodule at the level of carina (arrow). Axial fusion image (d) shows low-grade flurodeoxyglucose uptake in the endobronchial nodule (arrow) and intense uptake in flurodeoxyglucose emboli (arrowhead). Histopathological examination revealed schwannoma

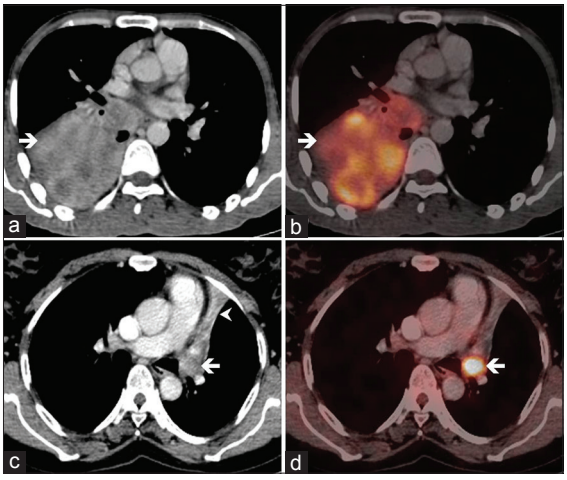

Figure 10: Inflammatory myofibroblastic tumor: A 34-year-old man with complaints of cough. Axial computed tomography (a) shows a heterogeneously enhancing soft-tissue mass with necrotic areas in the right lung (arrow). Axial fusion image (b) shows intense flurodeoxyglucose uptake in the right lung mass (arrow). Histopathologic examination revealed inflammatory myofibroblastic tumor. Endobronchial inflammatory myofibroblastic tumor: A 42-year-old woman with complaints of dyspnea. Axial computed tomography (c) shows endobronchial soft-tissue in the left upper lobe bronchus (arrow) with distal collapse (arrowhead). Axial fusion image (d) shows flurodeoxyglucose uptake in the endobronchial nodule (arrow). Histopathology revealed inflammatory myofibroblastic tumor

Solitary Fibrous Tumor

Solitary fibrous tumor of the lung is a benign or malignant spindle cell neoplasm of fibroblastic or myofibroblastic origin that commonly arises in the pleura. On CT, small tumors appear as hyperdense, well-defined mass lesions forming obtuse angles with the pleura and show homogeneous enhancement. Large tumors may undergo necrosis, hemorrhage, cystic degeneration, and calcification and appear heterogeneous with similar enhancement pattern.[24] On FDG PET, these tumors usually show heterogeneous and low-grade uptake similar to mediastinal blood pool [Figure 11]. Few studies have shown that the uptake patterns vary in benign and malignant fibrous tumors and thus aid in the differentiation.[25]

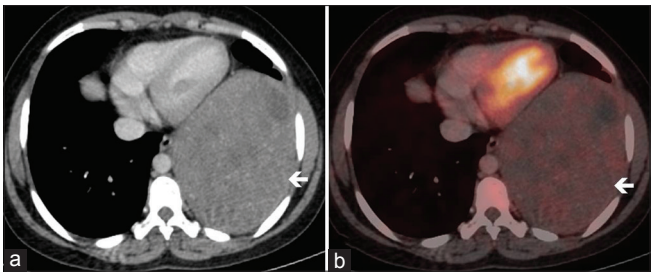

Figure 11: Solitary fibrous tumor: A 41-year-old woman with complaints of dyspnea and chest pain. Axial computed tomography image (a) shows a large heterogeneously enhancing soft-tissue mass in the left lung with necrotic areas (arrow). Axial fusion image (b) shows very low-grade flurodeoxyglucose uptake in the left lung mass (arrow). Histopathologic examination revealed spindle cell tumor, consistent with solitary fibrous tumor

Perivascular Epithelioid Cell Tumor

Perivascular epithelioid cell tumors (PEComas) are rare mesenchymal neoplasms composed of epithelioid or spindle cells in perivascular location. They are frequently benign and are cured with surgical resection. However, malignant cases are reported, which show local recurrence or distant metastases.[26] They are also referred as clear cell sugar tumors of the lung and usually present as a solitary peripheral lung nodule that is well defined spherically with no evidence of calcification or cavitation. These lesions have good vascular supply and enhance brilliantly on contrast administration.[27] Benign PEComas show low-grade FDG uptake. Malignant PEComas have upregulation of mTOR pathway which controls multiple cellular processes including GLUT-1, and these lesions show high FDG uptake [Figure 12].[28]

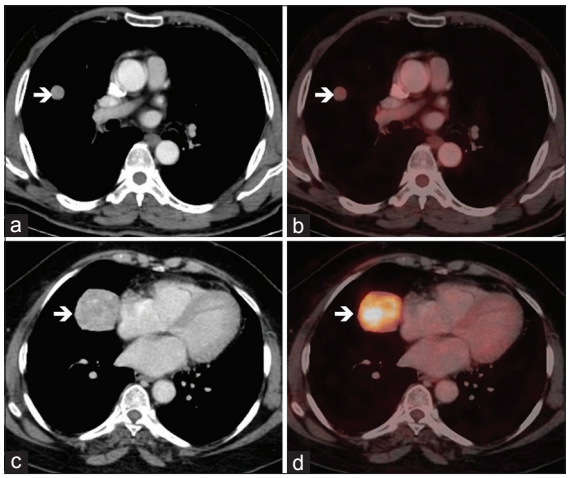

Figure 12: Benign perivascular epithelioid cell tumor: A 70-year-old man with incidental right lung nodule. Axial computed tomography (a) shows solitary right lung nodule (arrow). Axial fusion image (b) shows low-grade flurodeoxyglucose uptake in the right lung nodule (arrow). Histopathology revealed primary benign perivascular epithelioid cell tumor of lung. Malignant perivascular epithelioid cell tumor: A 51-year-old woman with complaints of cough. Axial computed tomography (c) shows a heterogeneously enhancing right lung mass (arrow). Axial fusion image (d) shows flurodeoxyglucose concentration in the right lung mass (arrow). Histopathology showed aggressive histological features favoring malignant perivascular epithelioid cell tumor. The flurodeoxyglucose uptake is significantly high in malignant perivascular epithelioid cell tumor

Pleomorphic Adenoma of Lung

Pleomorphic adenoma is a common benign neoplasm occurring in the salivary glands. It rarely arises in the trachea and is more uncommon to occur in lung parenchyma. Primary pulmonary pleomorphic adenoma has similar histopathologic features as salivary gland pleomorphic adenomas.[29] The imaging characteristics of primary pulmonary pleomorphic adenomas are not adequately described and on imaging, these tumors may be confused with other primary or metastatic lung tumors. On CT scan, it may appear as homogeneous, circular, soft-tissue density nodule or mass lesions with smooth margins in the peripheral lung parenchyma.[30] On FDG PET, these lesions show low-grade FDG uptake similar to other benign neoplasms [Figure 13].[29]

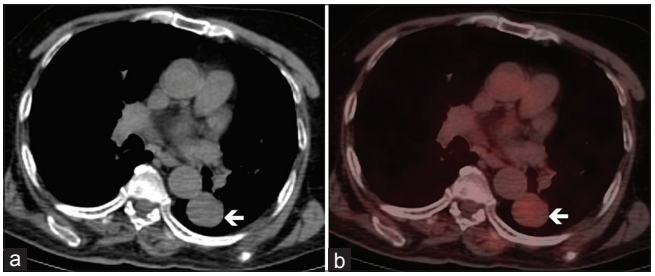

Figure 13: Primary pleomorphic adenoma of lung: A 75-year-old man with incidentally detected left lung nodule. Axial computed tomography image (a) shows homogeneous soft-tissue nodule in the left lung (arrow). Axial fusion image (b) shows very low-grade flurodeoxyglucose uptake in the left lung nodule (arrow). Histopathologic examination revealed primary pleomorphic adenoma of lung

Carcinoid

Carcinoid tumor arises from the neuroendocrine cells of the bronchial mucosa. Endobronchial tumors are a more common presentation compared to parenchymal nodules.[31] On CT, they appear as spherical or ovoid, well-defined, homogeneous nodules or mass lesions. Narrowing or obstruction of the bronchus can occur resulting in atelectasis, bronchiectasis, or obstructive

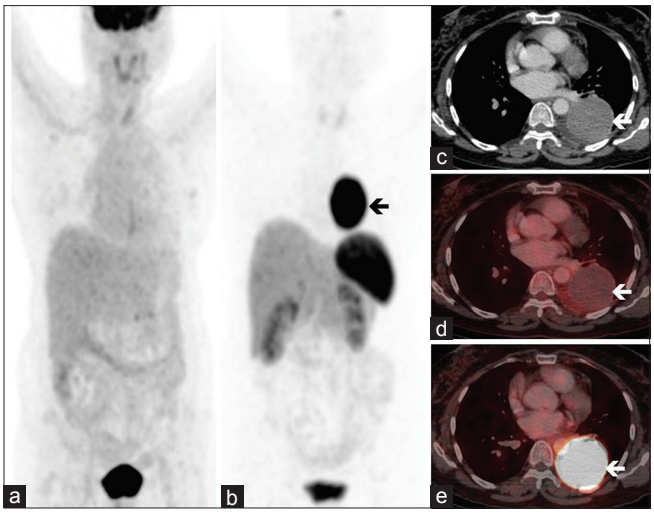

Figure 14: Typical carcinoid: A 56-year-old woman with hemoptysis. 18F flurodeoxyglucose positron emission tomography-computed tomography whole-body maximum intensity projection image (a) shows no abnormal tracer concentration. Axial computed tomography image (c) shows an enhancing soft-tissue mass in the left lung (arrow). Axial fusion image of flurodeoxyglucose positron emission tomography-computed tomography (d) shows no flurodeoxyglucose uptake in the left lung mass (arrow). 68Ga DOTANOC positron emission tomography-computed tomography whole-body maximum intensity projection image (b) shows intense tracer uptake in the left thorax (arrow). Axial fusion image of 68Ga DOTANOC positron emission tomography-computed tomography (e) shows intense tracer uptake in the left lung mass (arrow). Histopathologic examination revealed typical carcinoid

pneumonia. On contrast administration, these lesions shows good enhancement as they have abundant vascular supply. Typical carcinoids which are more commonly seen compared to the atypical variant are more indolent and have low glucose turnover and usually show less FDG uptake.[32] However, these tumors express somatostatin receptors, and radiolabeled somatostatin analog such as 68 gallium DOTANOC shows excellent concentration in these tumors, which aids in the diagnosis [Figure 14].[33]

Castleman Disease

Castleman disease (CD), also known as angiofollicular hyperplasia or giant lymph node hyperplasia, is a benign lymphoproliferative disorder. It can be clinicoradiogically classified as unicentric (unifocal) or multicentric (multifocal). Approximately 70% of CD occurs in the thorax and commonly manifests as a mediastinal or hilar mass. In unicentric disease, CT generally shows well-circumscribed homogeneous mass lesions.[34] Interleukin-6-induced inflammation is the major pathophysiological mechanism for CD and on FDG PET-CT, these lesions show moderately increased uptake.[35] A hilar soft-tissue mass with FDG uptake can mimic bronchogenic carcinoma [Figure 15].

Conclusion

Benign and low-grade malignant tumors may pose a diagnostic challenge on imaging. The morphologic and metabolic characteristics of these tumors often show significant overlap with malignant lesions. Awareness of the common mimics of lung cancer and a thorough understanding of their key imaging characteristics on CT as well as FDG PET is helpful in narrowing the differential diagnosis, eventually leading to prompt and appropriate treatment.

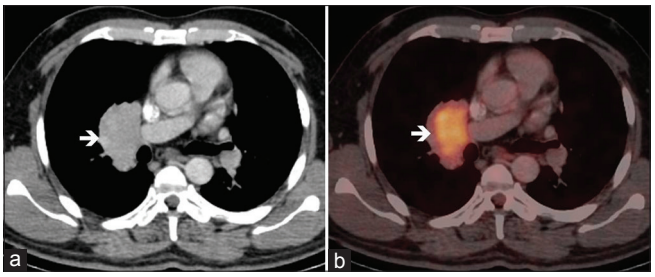

Figure 15: Castleman disease: A 40-year-old man with incidentally detected right hilar mass. Axial computed tomography image (a) shows homogeneous soft-tissue mass in the right lung near hilum (arrow). Axial fusion image (b) shows flurodeoxyglucose uptake in the right hilar mass (arrow). Histopathologic examination revealed reactive lymphoid tissue with atretic germinal centers consistent with Castleman disease

Declaration of patient consent

The authors certify that they have obtained all appropriate patient consent forms. In the form the patient(s) has/have given his/her/their consent for his/her/their images and other clinical information to be reported in the journal. The patients understand that their names and initials will not be published and due efforts will be made to conceal their identity, but anonymity cannot be guaranteed.

Financial support and sponsorship

Nil.

Conflicts for interest

There are no conflicts for interest.

References

1. Madsen PH, Holdgaard PC, Christensen JB, Høilund-Carlsen PF. Clinical utility of F-18 FDG PET-CT in the initial evaluation of lung cancer. Eur J Nucl Med Mol Imaging 2016;43:2084-97.
2. Nachiappan AC, Rahbar K, Shi X, Guy ES, Mortani Barbosa EJ Jr., Shroff GS, *et al.* Pulmonary tuberculosis: Role of radiology in diagnosis and management. Radiographics 2017;37:52-72.
3. Yang CM, Hsu CH, Lee CM, Wang FC. Intense uptake of [F-18]-fluoro-2 deoxy-D-glucose in active pulmonary tuberculosis. Ann Nucl Med 2003;17:407-10.
4. Yang PS, Lee KS, Han J, Kim EA, Kim TS, Choo IW. Focal organizing pneumonia: CT and pathologic findings. J Korean Med Sci 2001;16:573-8.
5. Erdoğan Y, Özyürek BA, Özmen Ö, Yılmaz Demirci N, Duyar SŞ, Dadalı Y, *et al.* The evaluation of FDG PET/CT scan findings in patients with organizing pneumonia mimicking lung cancer. Mol Imaging Radionucl Ther 2015;24:60-5.
6. Criado E, Sánchez M, Ramírez J, Arguis P, de Caralt TM, Perea RJ, *et al.* Pulmonary sarcoidosis: Typical and atypical manifestations at high-resolution CT with pathologic correlation. Radiographics 2010;30:1567-86.

7. Mostard RL, Vöö S, van Kroonenburgh MJ, Verschakelen JA, Wijnen PA, Nelemans PJ, *et al.* Inflammatory activity assessment by F18 FDG-PET/CT in persistent symptomatic sarcoidosis. Respir Med 2011;105:1917-24.
8. Franquet T, Müller NL, Giménez A, Guembe P, de La Torre J, Bagué S. Spectrum of pulmonary aspergillosis: Histologic, clinical, and radiologic findings. Radiographics 2001;21:825-37.
9. Baxter CG, Bishop P, Low SE, Baiden-Amissah K, Denning DW. Pulmonary aspergillosis: An alternative diagnosis to lung cancer after positive [18F] FDG positron emission tomography. Thorax 2011;66:638-40.
10. Nam BD, Kim TJ, Lee KS, Kim TS, Han J, Chung MJ. Pulmonary mucormycosis: Serial morphologic changes on computed tomography correlate with clinical and pathologic findings. Eur Radiol 2018;28:788-95.
11. Dang CJ, Li YJ, Zhan FH, Shang XM. The appearance of pulmonary mucormycosis on FDG PET/CT. Clin Nucl Med 2012;37:801-3.
12. Martinez F, Chung JH, Digumarthy SR, Kanne JP, Abbott GF, Shepard JA, *et al.* Common and uncommon manifestations of Wegener granulomatosis at chest CT: Radiologic-pathologic correlation. Radiographics 2012;32:51-69.
13. Ananthakrishnan L, Sharma N, Kanne JP. Wegener's granulomatosis in the chest: High-resolution CT findings. AJR Am J Roentgenol 2009;192:676-82.
14. De Geeter F, Gykiere P. (18) F-FDG PET/CT imaging in granulomatosis with polyangiitis. Hell J Nucl Med 2016;19:5-6.
15. Bolca N, Topal U, Bayram S. Bronchopulmonary sequestration: Radiologic findings. Eur J Radiol 2004;52:185-91.
16. Li X, He W, Li J, Ouyang R, Chen P, Peng H, *et al.* Pulmonary sequestration associated with increased serum tumor markers and elevated standard uptake value level in PET/CT: A case report and literature review. Medicine (Baltimore) 2018;97:e11714.
17. Park CM, Goo JM, Lee HJ, Kim MA, Lee CH, Kang MJ. Tumors in the tracheobronchial tree: CT and FDG PET features. Radiographics 2009;29:55-71.
18. Pavlus JD, Carter BW, Tolley MD, Keung ES, Khorashadi L, Lichtenberger JP 3rd. Imaging of thoracic neurogenic tumors. AJR Am J Roentgenol 2016;207:552-61.
19. Shimada Y, Sawada S, Hojo S, Okumura T, Nagata T, Nomoto K, *et al.* Glucose transporter 3 and 1 may facilitate high uptake of 18F-FDG in gastric schwannoma. Clin Nucl Med 2013;38:e417-20.
20. Furuya K, Yasumori K, Takeo S, Sakino I, Uesugi N, Momosaki S, *et al.* Lung CT: Part 1, mimickers of lung cancer – Spectrum of CT findings with pathologic correlation. AJR Am J Roentgenol 2012;199:W454-63.
21. Wang W, Song J, Shi J, Hu H, Wu Y, Yan J, *et al.* Slight uptake of 18F-FDG on positron emission tomography in pulmonary hamartoma: A case report. Oncol Lett 2015;10:430-2.
22. Giménez A, Franquet T, Prats R, Estrada P, Villalba J, Bagué S. Unusual primary lung tumors: A radiologic-pathologic overview. Radiographics 2002;22:601-19.
23. Huellner MW, Schwizer B, Burger I, Fengels I, Schläpfer R, Bussmann C, *et al.* Inflammatory pseudotumor of the lung with high FDG uptake. Clin Nucl Med 2010;35:722-3.
24. Rosado-de-Christenson ML, Abbott GF, McAdams HP, Franks TJ, Galvin JR. From the archives of the AFIP: Localized fibrous tumor of the pleura. Radiographics 2003;23:759-83.
25. Cardillo G, Carbone L, Carleo F, Masala N, Graziano P, Bray A, *et al.* Solitary fibrous tumors of the pleura: An analysis of 110 patients treated in a single institution. Ann Thorac Surg 2009;88:1632-7.
26. Tirumani SH, Shinagare AB, Hargreaves J, Jagannathan JP, Hornick JL, Wagner AJ, *et al.* Imaging features of primary and metastatic malignant perivascular epithelioid cell tumors. AJR Am J Roentgenol 2014;202:252-8.
27. Santana AN, Nunes FS, Ho N, Takagaki TY. A rare cause of hemoptysis: Benign sugar (clear) cell tumor of the lung. Eur J Cardiothorac Surg 2004;25:652-4.
28. Sun L, Sun X, Li Y, Xing L. The role of (18) F-FDG PET/CT imaging in patient with malignant PEComa treated with mTOR inhibitor. Onco Targets Ther 2015;8:1967-70.
29. Nakamura A, Takuwa T, Kondo N, Watanabe T, Hirota S, Hasegawa S. A rare case of pleomorphic adenoma with difficult diagnosis using biopsy. J Thorac Dis 2018;10:E630-3.
30. Kanchustambham V, Saladi S, Patolia S, Mahmoud Assaf S, Stoeckel D. A rare case of a benign primary pleomorphic adenoma of the lung. Cureus 2017;9:e1069.
31. Meisinger QC, Klein JS, Butnor KJ, Gentchos G, Leavitt BJ. CT features of peripheral pulmonary carcinoid tumors. AJR Am J Roentgenol 2011;197:1073-80.
32. Moore W, Freiberg E, Bishawi M, Halbreiner MS, Matthews R, Baram D, *et al.* FDG-PET imaging in patients with pulmonary carcinoid tumor. Clin Nucl Med 2013;38:501-5.
33. Kayani I, Conry BG, Groves AM, Win T, Dickson J, Caplin M, *et al.* A comparison of 68Ga-DOTATATE and 18F-FDG PET/CT in pulmonary neuroendocrine tumors. J Nucl Med 2009;50:1927-32.
34. Luo JM, Li S, Huang H, Cao J, Xu K, Bi YL, *et al.* Clinical spectrum of intrathoracic Castleman disease: A retrospective analysis of 48 cases in a single Chinese hospital. BMC Pulm Med 2015;15:34.
35. Lee ES, Paeng JC, Park CM, Chang W, Lee WW, Kang KW, *et al.* Metabolic characteristics of Castleman disease on 18F-FDG PET in relation to clinical implication. Clin Nucl Med 2013;38:339-42.t